

Validation Study of Multi-Rotor Systems Using Two Shrouded Wind Turbines

Halawa, Amr M.

Wind Engineering Division, Research Institute for Applied Mechanics, Kyushu University

Uchida, Takanori

Wind Engineering Division, Research Institute for Applied Mechanics, Kyushu University

Watanabe, Koichi

Renewable Energy Utilization Unit, Kyushu University Platform of Inter/Transdisciplinary Energy Research

Ohya, Yuji

Wind Engineering Division, Research Institute for Applied Mechanics, Kyushu University

<https://hdl.handle.net/2324/4476144>

出版情報 : Journal of Physics: Conference Series. 1618 (032017), 2020-09-21. IOP Publishing
バージョン :

権利関係 : Creative Commons Attribution 3.0 International



PAPER • OPEN ACCESS

Validation Study of Multi-Rotor Systems Using Two Shrouded Wind Turbines

To cite this article: Amr M. Halawa *et al* 2020 *J. Phys.: Conf. Ser.* **1618** 032017

View the [article online](#) for updates and enhancements.



IOP | ebooks™

Bringing together innovative digital publishing with leading authors from the global scientific community.

Start exploring the collection—download the first chapter of every title for free.

Validation Study of Multi-Rotor Systems Using Two Shrouded Wind Turbines

Amr M. Halawa¹, Takanori Uchida¹, Koichi Watanabe², and Yuji Ohya¹

¹ Wind Engineering Division, Research Institute for Applied Mechanics, Kyushu University, Japan

² Renewable Energy Utilization Unit, Kyushu University Platform of Inter/Transdisciplinary Energy Research, Japan

E-mail: amrhalawa@kyudai.jp

Abstract. Multi rotor systems (MRS) have shown a great potential as a future application of wind energy. In this study, the aim is simulating the aerodynamic performance of a an MRS using fully-resolved shrouded wind turbine blades then validating with experimental data. MRS for wind turbine configurations have been studied using both numerical and experimental approaches. Different case studies have been studied and the power output comparison have been reported. The wind lens turbine (WLT) obviously shows a large increase in power output compared to the bare rotor case. Besides, the twin side-by-side (SBS) WLTs shows even larger power increase compared to the case of single WLT by around 20% for computational fluid dynamics (CFD) calculations at the optimum tip speed ratio s/D of around 0.2. The increase in power coefficient in close proximity can be explained by flow interference and gap flow behaviors. Previously, we used simplified models for blade modeling like actuator line method (ALM) and actuator disk method (ADM). However, currently we are improving the accuracy using CFD with full-scale blades with higher grid resolutions. As the number of units for an MRS is increased, the increase in power output becomes larger and larger. This is because that the gap flows between brimmed diffuser-augmented wind turbines (B-DAWT) in a MRS are accelerated and cause lowered pressure regions due to vortex interaction behind the brimmed diffusers. Thus, an MRS with more B-DAWTs can draw more wind into turbines showing higher power output.

1. Introduction

Wind power energy is obviously attracting attention as having a great source of green energy. The global mainstream trend of wind turbines is increasing their size to achieve higher output power. However, as the scale of the wind turbine gets bigger, the cost is getting higher, and the failure rate becomes larger due to associated instability and aeroelasticity problems. Therefore, multi-rotors are a promising application in this perspective. Advantages of multirotor systems (MRSs) concepts have been suggested by Jamieson and Branney [1,6-7]. This system consists of many small or medium sized wind turbines in the same vertical plane with small gaps supported by one tower [2]. Some of the merits of MRS can be summarized as follows: a great reduction in weight, great reduction in cost consequently mass production of turbine unit. If we apply the Wind-Lens turbine to MRS, we can expect 10 – 20% increase in total power output due to the unique mechanism of Wind-Lens. Some of the studies of MRS that have been



Content from this work may be used under the terms of the [Creative Commons Attribution 3.0 licence](https://creativecommons.org/licenses/by/3.0/). Any further distribution of this work must maintain attribution to the author(s) and the title of the work, journal citation and DOI.

published so far covered wind tunnel experiments, numerical simulations, and field experiments [3–16]. In order to increase the rotor performance of a conventional wind turbine, Diffuser-Augmented Wind Turbines (DAWTs) have been developed. The aerodynamics of brimmed diffuser-augmented wind turbines (B-DAWT), named "wind-lens turbine, (WLT)" has been investigated. Generally, a WLT is composed of a downwind type wind turbine and a structure composed of an inlet shroud, a diffuser, and a brim. Vortices are generated behind the structure from the flow passing inside the diffuser and that behind the brim. Consequently, a low pressure region is created behind the turbine by the vortices shedding. Thus, more air is drawn into the turbine at a higher accelerated speed compared to the case of a conventional wind turbine (i.e. with no diffuser). In the present research, we have studied single and twin WLTs in closely spaced array using wind tunnel experiments and a RANS based on a finite volume method (FVM). The results show that remarkable increase in total power output. To investigate more about the power increase for each studies case of WLTs configuration, measurements of wind velocity and static pressure distributions at the three locations behind the WLTs are made and compared to CFD calculations for the same locations and configurations. RANS calculations validate the results from wind tunnel experiments and provide a better understanding of the flow interference among WLTs as will be shown in the following sections.

2. Methodology

In our work, we solved the problem from both an experimental and numerical approaches as explained in the following subsections.

2.1. Experimental Approach

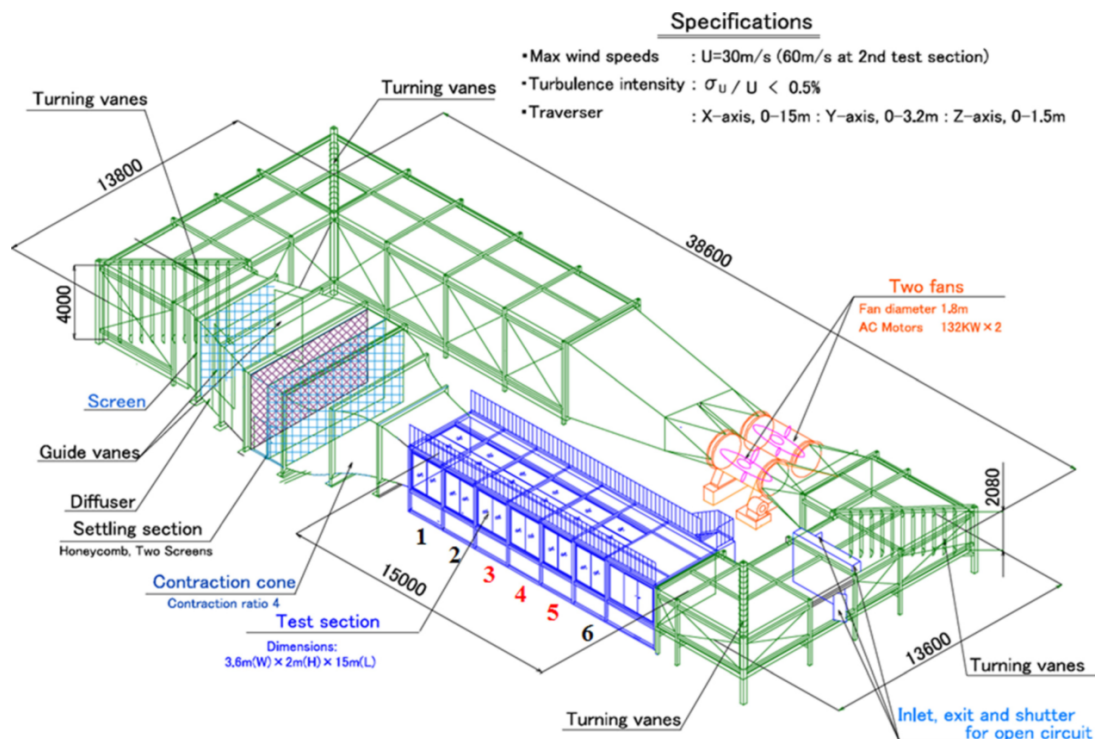


Figure 1: Boundary-layer wind tunnel, Kyushu University [19]

For the experimental part, the large boundary-layer wind tunnel of the Research Institute for Applied Mechanics, Kyushu University, was used. The wind tunnel has a measurement section of

15m long \times 3.6m wide \times 2m high with a maximum wind velocity of 30 m/s and is characterized by a low turbulence intensity of 0.4% [19] as shown in Figure 1.

To reduce the blockage effects, the side walls and ceiling panels surrounding the test section have been removed. From a total of 6 potential sections, the third to fifth sections are removed to create a 6 m opening on the side walls, thus making it a semi-open wind tunnel. A separate study was made to ensure the mitigation of wind tunnel blockage effects [17]. The paper showed experimental results of five rotors where the experimental results had good agreement with numerical results. Thus, our semi-open wind tunnel could mitigate blockage effect to such a level even if the MRS had five rotors. Consequently, it is guaranteed for the twin side-by-side WLTs configuration.

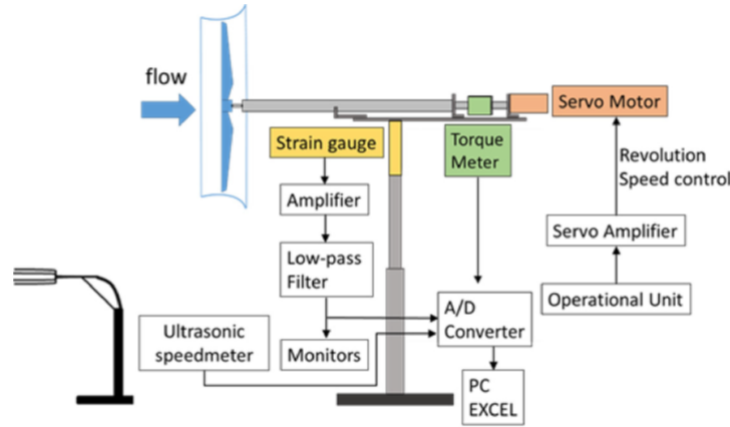


Figure 2: Schematic of the measurement system for the power output [17]

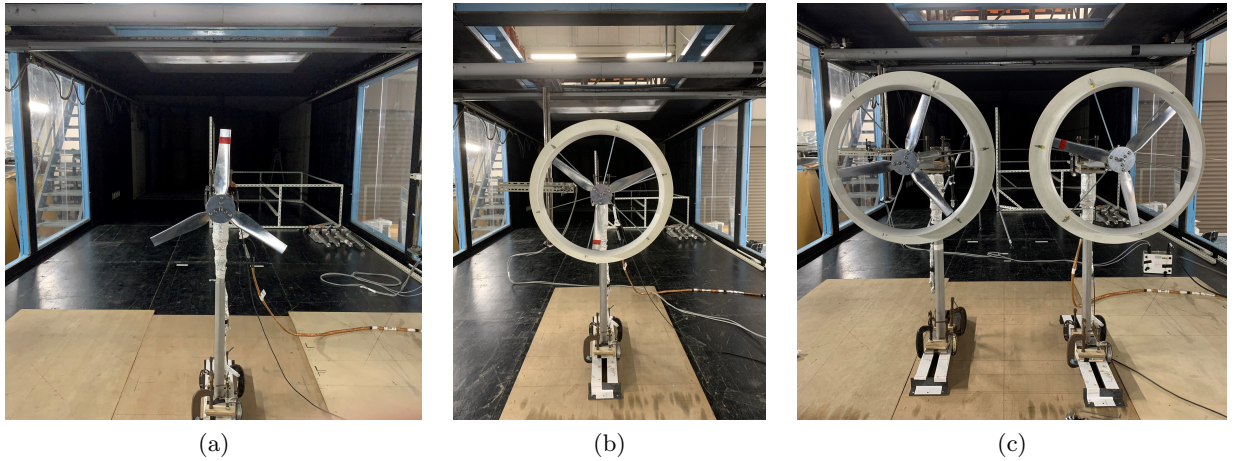
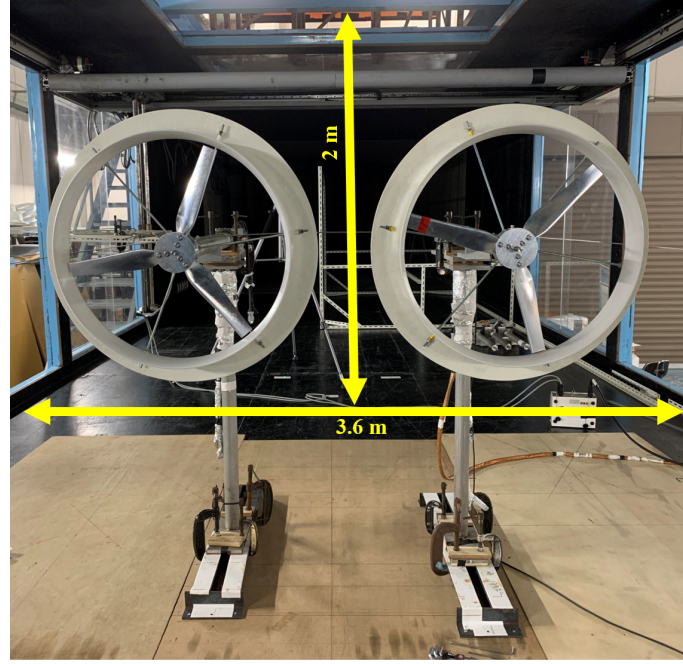


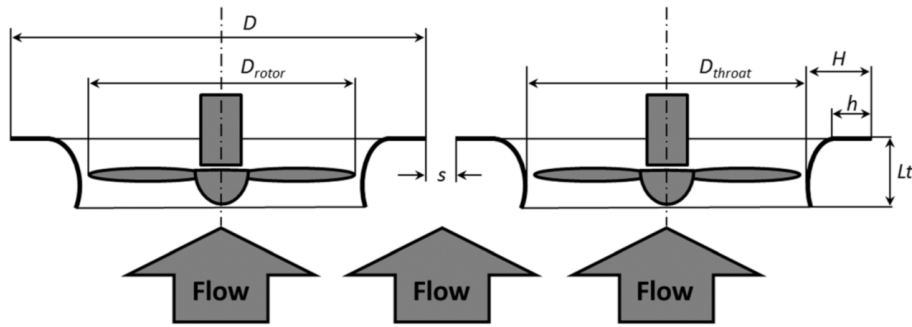
Figure 3: Experimental configurations for: Bare rotor (a) , Single WLT (b), and Two SBS WLTs (c)

Experiments were done on a bare rotor, then one shrouded wind lens turbine (WLT) configuration, and two WLTs configuration in a Side-By-Side (SBS) arrangement as shown in Figures 1-4. For the MRS experiments, a schematic of the dimensions of the WLT configuration in a SBS arrangement, including the shape of the shroud (brimmed diffuser) with brim height of h . The brimmed diffuser of the WLT consists of a diffuser with a streamwise length $L_t = 0.22D_{throat}$ and a brim height $h = 0.075D_{throat}$, called CüB7.5 type WLT [21]. Two WLTs are placed in SBS arrangements with gap width s for the two WLT configuration 3. The

representative diameter of a WLT is D , i.e., $D = D_{brim}$. In the present experiments, the gap ratio is s/D . The rotor diameter D_{rotor} of the turbine model is 442mm . The approaching wind speed is 14m/s with a Reynolds numbers of 4.2×10^5 with respect to the rotor diameter D_{rotor} . The rotor blades were manufactured using a computer numerical control machine (CNC), and have cross sections corresponding to MEL-type aerofoils [22].



(a)



(b)

Figure 4: Wind tunnel setup (a) and schematic of the dimensions of the WLT configuration in an SBS arrangement (b) [19]

In order to measure the the output power, the torque is needed to be calculated firstly. Figure 2 shows a torque meter connected to the rotor shaft and the motor. The torque $T_r(Nm)$ and the rotational speed $f(Hz)$ of the wind turbine are measured for $30s$ at $1kHz$ sampling frequency, at a constant servomotor rotational velocity, in the condition that the turbine loading was gradually applied from zero. The output power is calculated as $P(W) = T_r \times 2\pi f$ and shown as a performance curve. It is worth noting that the directions of rotation of all the turbines in all studied configurations are in a clockwise direction from an upstream point of view. All the measured data are fed into a PC using an AD-Converter. The optimum tip speed ratio λ

is determined by setting the appropriate rotational speed of the rotor. For the measurement period, the motor speed is held constant by the servomotor controller. In general, the power coefficient C_p of a turbine is evaluated using Equation 1:

$$C_p = \frac{P_{turbine}}{\frac{1}{2}\rho U_o^3 A} = \frac{T_r \omega}{\frac{1}{2}\rho U_o^3 A} \quad (1)$$

where A is the swept area of the rotor for both the conventional turbine and WLT. The maximum power coefficient, $C_{P_{0i}}$ of each turbine in stand-alone configurations is measured at their optimum tip speed ratio λ .

In this specific experiment, the experimental drag force (thrust force) F_{drag} was not measured due to some wind tunnel reservation limitations, however an extensive study was done before by Ohya et al. [19]. It was found that for two WLTs, the optimum spacing ratio s/D is 0.2, thus in the current experiment and simulations, the optimum s/D value was used. Sample data are shown later in the Results section. Furthermore, various tip speed ratios λ were tested where the optimum one was found to be of value 3.5.

On the other hand, in order to measure velocity distribution in the turbine wake, an ultrasonic speedometer was used as shown in Figure 2. This sensor was moved by a traversing system. The u -velocity fluctuation was measured with sampling frequency of 1000 Hz and sampling time of 30 s at each sampling point. Generally, the time-averaged nondimensional u -velocity is u/U_o , where U_o is the speed of the approaching flow.

2.2. Numerical Approach

For the numerical part, unlike the previously performed simulations using ALM & ADM with the in-house CFD code [17,18], fully resolved blades simulations were carried out using ANSYS Fluent CFD on a 16-core cluster as well as Kyushu University Supercomputer, ITO. Simulations were performed on multiple turbine configurations, starting with a single blade with cyclic symmetric boundaries using SRF model, then full rotor analysis, afterwards inserting the WLT and solving for single and double SBS cases using MRF model. Flow variables were calculated using three-dimensional RANS simulation based on the FVM in Cartesian coordinates. The governing equations are the continuity and Navier–Stokes equations. A first-order explicit method is used for time marching. A second-order upwind scheme is applied to the convective terms. The second-order central difference scheme is applied to the diffusion terms.

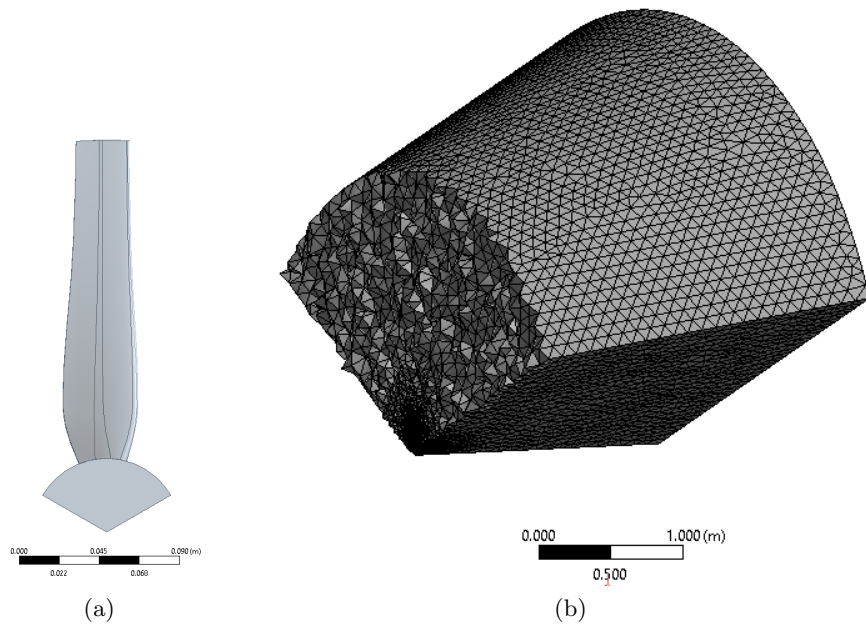


Figure 5: Single SRF rotor (a) and its corresponding computational grid (b)

To reduce any blockage effects, a large computational domain (around 3.5 million cells) is adopted, as described in Figures 5-7. For the preliminary case of SRF model, a RANS simulation was performed on a single blade of the rotor (due to symmetry) with the following configuration and computational domain as shown in Figure 5. Periodic boundary conditions were used to account for the symmetry and only third of the domain was considered as previously validated by Halawa et al. [20]. The simulations were carried out at an inlet velocity of 14 m/s and the optimum TSR of the WLT of 3.5.

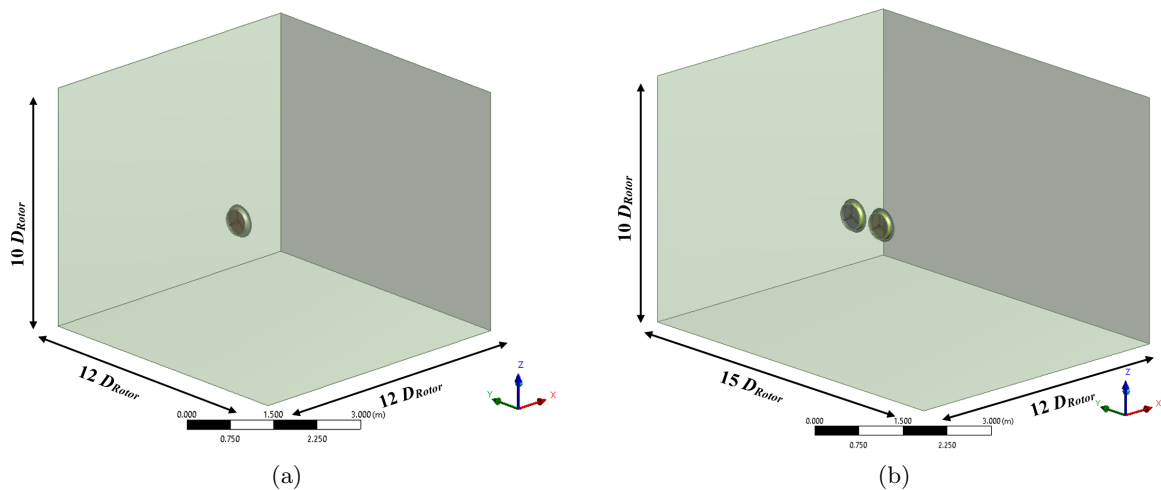


Figure 6: Computational MRF domain for a single WLT (a) and twin SBS WLTs (b)

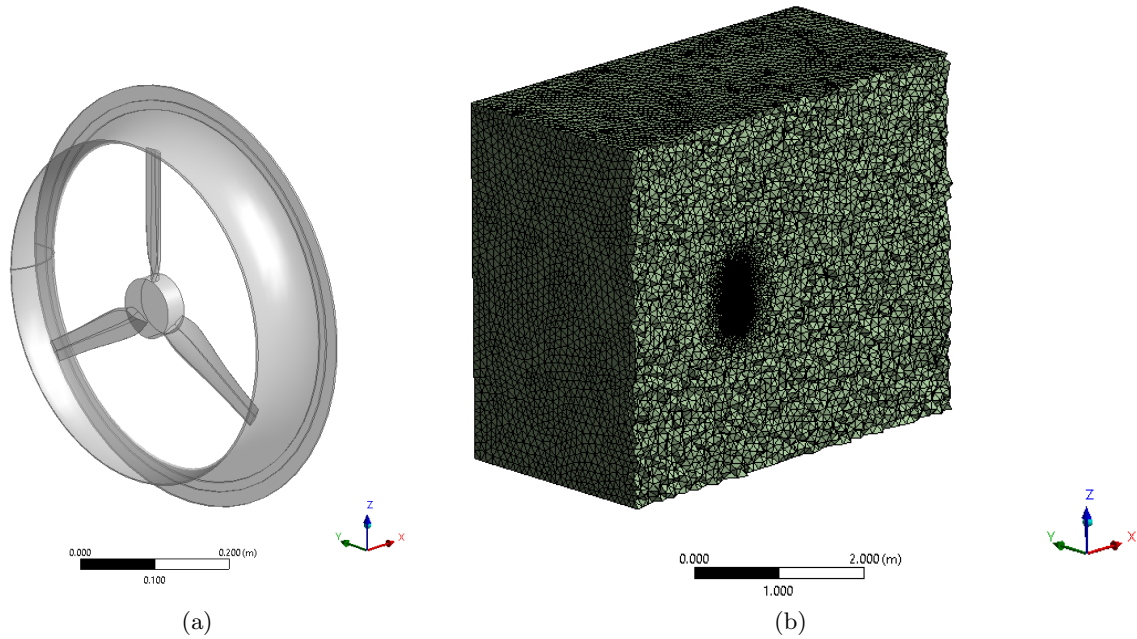


Figure 7: Current CiiB7.5 type WLT (a) and its corresponding computational grid (b)

The grid is refined near the turbines surface to capture the boundary layer effect as shown in Fig. 7. The computational were performed on a multi-core Linux cluster as well as Kyushu University Supercomputer ITO server. The current ANSYS license computational resources were quite challenging. The mesh needed to be finer to match the LES requirements, yet the license resources were limited. However, the overall tendency and qualitative results showed good agreements between the CFD simulations and the measurements from the wind tunnel experiments as will be shown later in the results section.

3. Results

3.1. Experimental Results

For the experimental part, from our previous experiment on the CiiB10 WLT type , the two-turbine configuration with WLTs in SBS arrangement in Figure 8-a shows an increase in the average power coefficient for all gap ratios s/D studied, as shown by the results of ΔC_p and ΔC_d in Figure 8-b. While the increase in power coefficient is notable for all gaps studied, the largest increase in ΔC_p , up to 8%, is achieved with the gap ratio at around $s/D = 0.2$. For the average drag coefficient ΔC_d , the largest increase is seen at around $s/D = 0.15-0.3$, reaching 5% [19]. Thus in our current study on the CiiB7.5 WLT type, the optimum $s/D = 0.2$ was used.

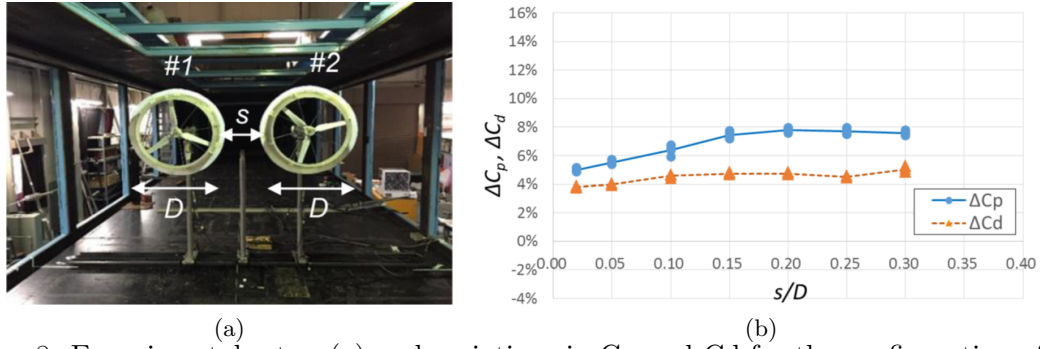


Figure 8: Experimental setup (a) and variations in C_p and C_d for the configuration of two WLTs in SBS arrangement, compared to those for the stand-alone configuration (b) [19]

For the current experimental study, various approaching wind speeds were studied. However, in our current validation study, we decided on the 14m/s . Figure 9 shows the experimental power coefficient distribution with tip speed ratio for all studied cases. Figure 9a depicts the experimental power coefficient for the bare rotor case and single WLT case while the twin SBS WLTs case is depicted in Figure 9b.

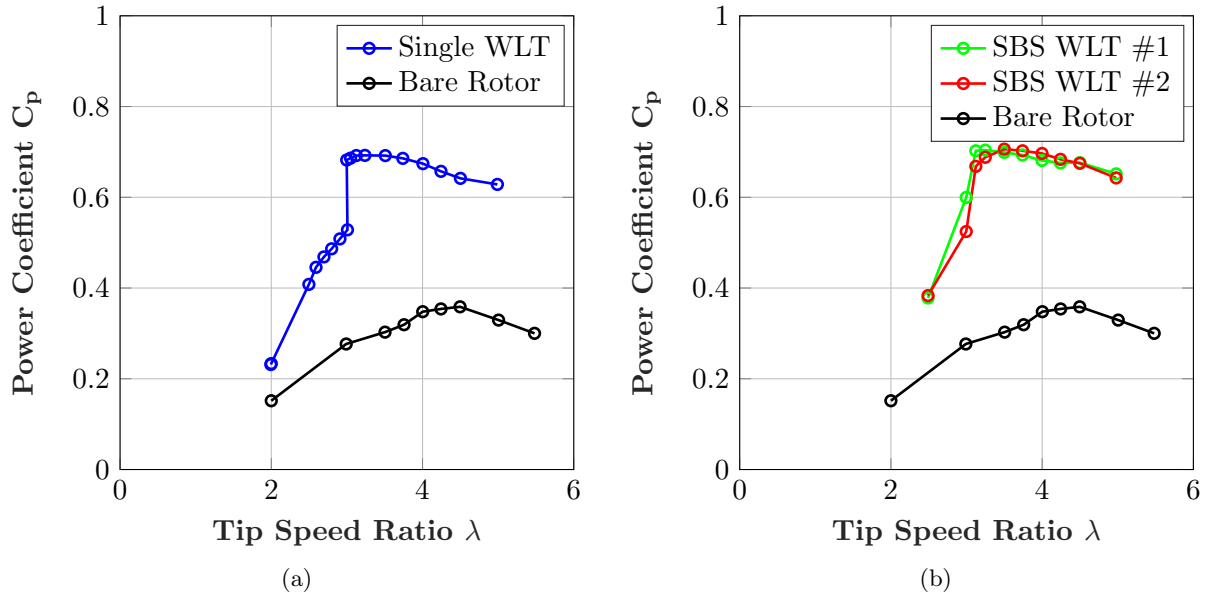
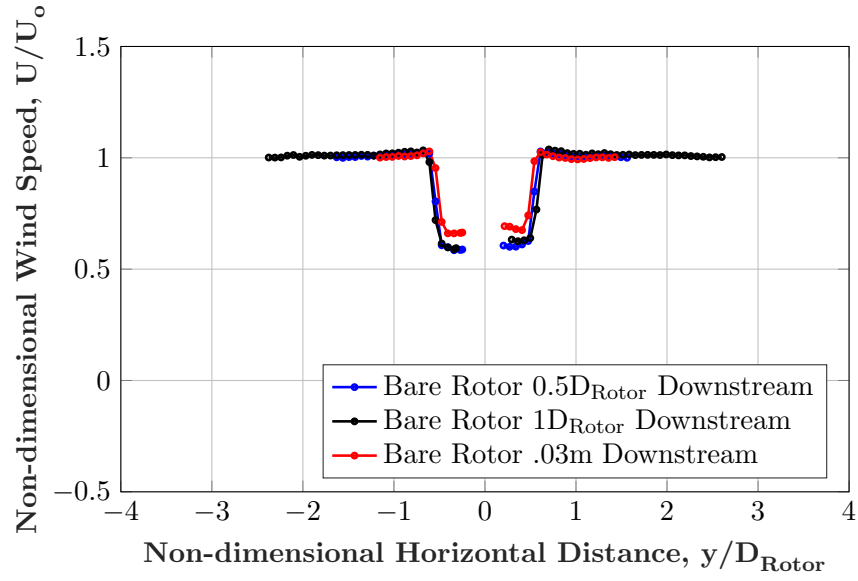
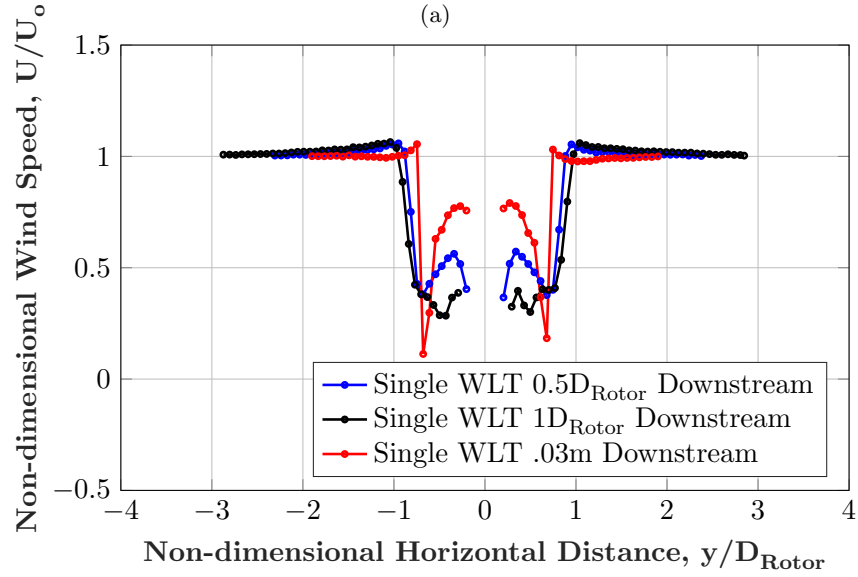


Figure 9: Experimental power coefficient distribution with tip speed ratio for bare rotor case and single WLT case (a), as well as twin SBS WLTs case (b)

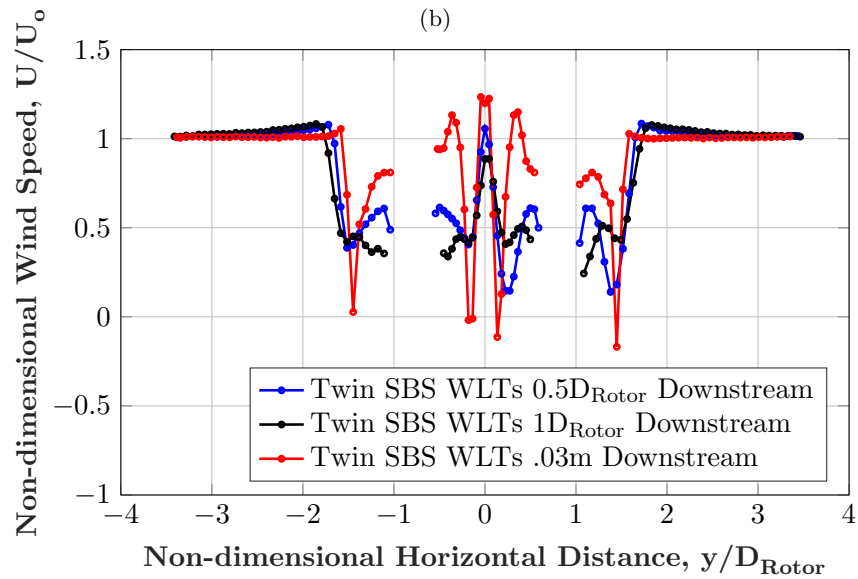
The experimental velocity distribution behind the turbines were measured at three different locations; right behind the rotor at $0.03m$, at a downstream distance of $0.5D_{Rotor}$ and at $1D_{Rotor}$ distance downstream as shown in Figure 10.



(a)



(b)



(c)

Figure 10: Comparisons of experimental u-velocity distributions at different downstream locations for bare rotor (a), single WLT (b), and twin SBS WLTs (c)

3.2. Numerical Results

For the numerical part, the results for the all the studies cases are shown as following. To visualize the flow, a cutting plane was constructed at the center height of the WLT as shown in Figure 11. Figures 12 shows an instantaneous flow around the simulated bare rotor, single WLT and twin SBS WLTs at $s/D = 0.2$. Figure 13 shows the instantaneous static pressure field. It is obvious that the streamwise velocity u in the gap region is larger than those in the surroundings, hence showing accelerated flow region. Correspondingly, a lowered pressure in the gap region is reflected in Figure 13. The accelerated gap flow is due to the flow interaction with the adjacent WLT.

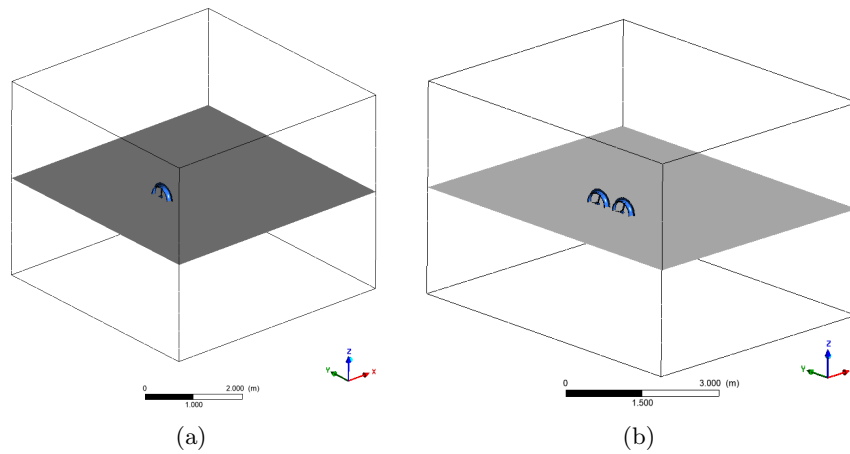


Figure 11: Visualization plane for single WLT (a), and twin SBS WLTs (b)

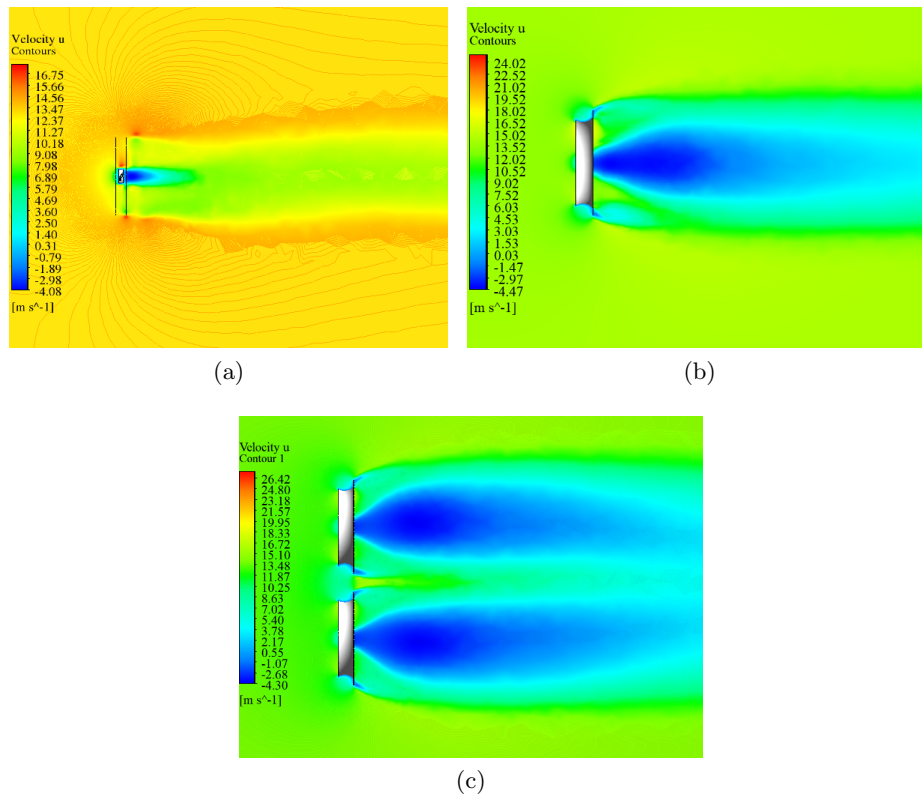


Figure 12: Instantaneous u -velocity field for the bare rotor (a), single WLT (b), and twin SBS WLTs (c), where flow is from left to right

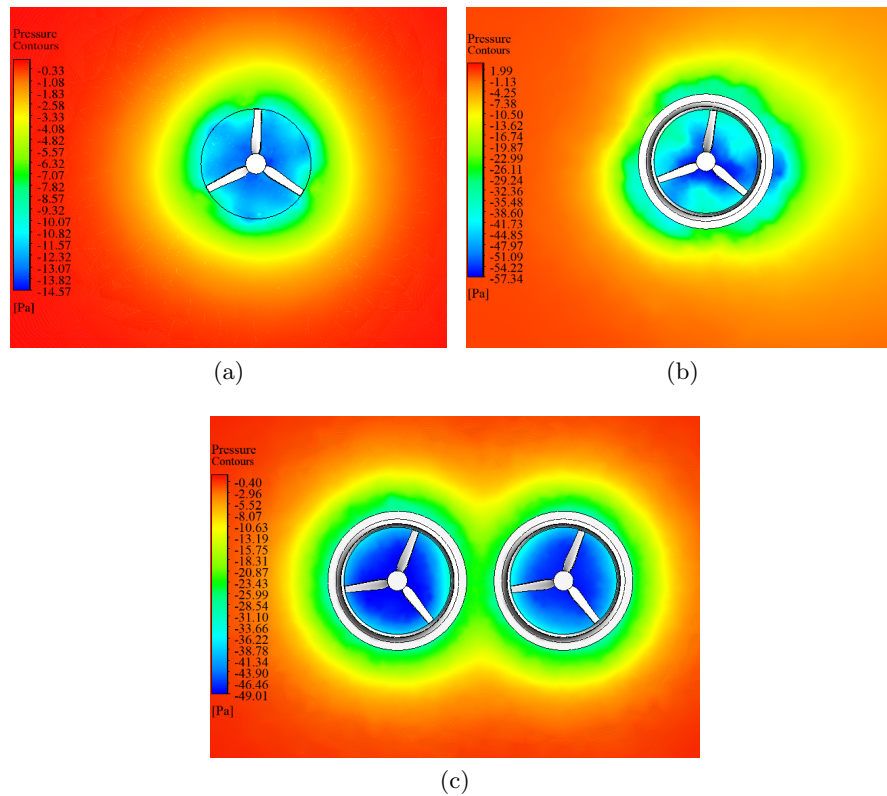


Figure 13: Instantaneous static pressure field for the bare rotor (a), single WLT (b), and twin SBS WLTs (c), evaluated at $0.4D_{Rotor}$ downstream

The numerical velocity distribution behind the turbines were calculated at three different locations; right behind the rotor at $0.03m$, at a downstream distance of $0.5D_{Rotor}$ and at $1D_{Rotor}$ distance downstream as shown in Figure 14. To validate the accuracy of CFD results, the numerical results are compared to those from the wind tunnel experiments, as shown in Figures 10, 14 and 15. Figure 15 shows the power output increase relative to the bare rotor for each case study of single WLT, and twin SBS WLTs $s/D = 0.2$ both for CFD and wind tunnel experiment. The WLT obviously shows a large increase in power output compared to the bare rotor case. Besides, the twin SBS WLTs shows even larger power increase compared to the case of single WLT by around 20% for CFD calculations. Figures 10 and 14 show the instantaneous u -velocity distributions along a horizontal line behind the turbines located at three different locations; right behind the rotor at $0.03m$, at a downstream distance of $0.5D_{Rotor}$ and at $1D_{Rotor}$ distance downstream. For the u -velocity distributions, the gap flows are strongly accelerated both in CFD and wind tunnel experiments, showing $u/U_o = 1.23$ and are in good agreement qualitatively. From Figures 10, 13 and 14, it can be concluded that pressure behind twin SBS WLTs is remarkably lowered compared to those for single WLT or bare rotor configurations. This can be explained by the accelerated gap flows effect that leads to vortices near the gaps, and thus causing the lowered pressure region behind the twin SBS WLTs. In other words, the lowered pressure region draws more airflow into the turbines in the MRS compared to the single WLT or bare rotor. Therefore, the power and drag values for MRS are higher compared to those of the stand-alone configurations. The increase in the power coefficient and the drag coefficient for MRS configuration in the close proximity can also be explained by the flow interference around bluff bodies and gap flow behaviors [23-24]. Reference [25] shows some similarities between the flow around three-dimensional bluff bodies (e.g. circular plates) in SBS arrangements and the flow around multiple WLTs in SBS configuration.

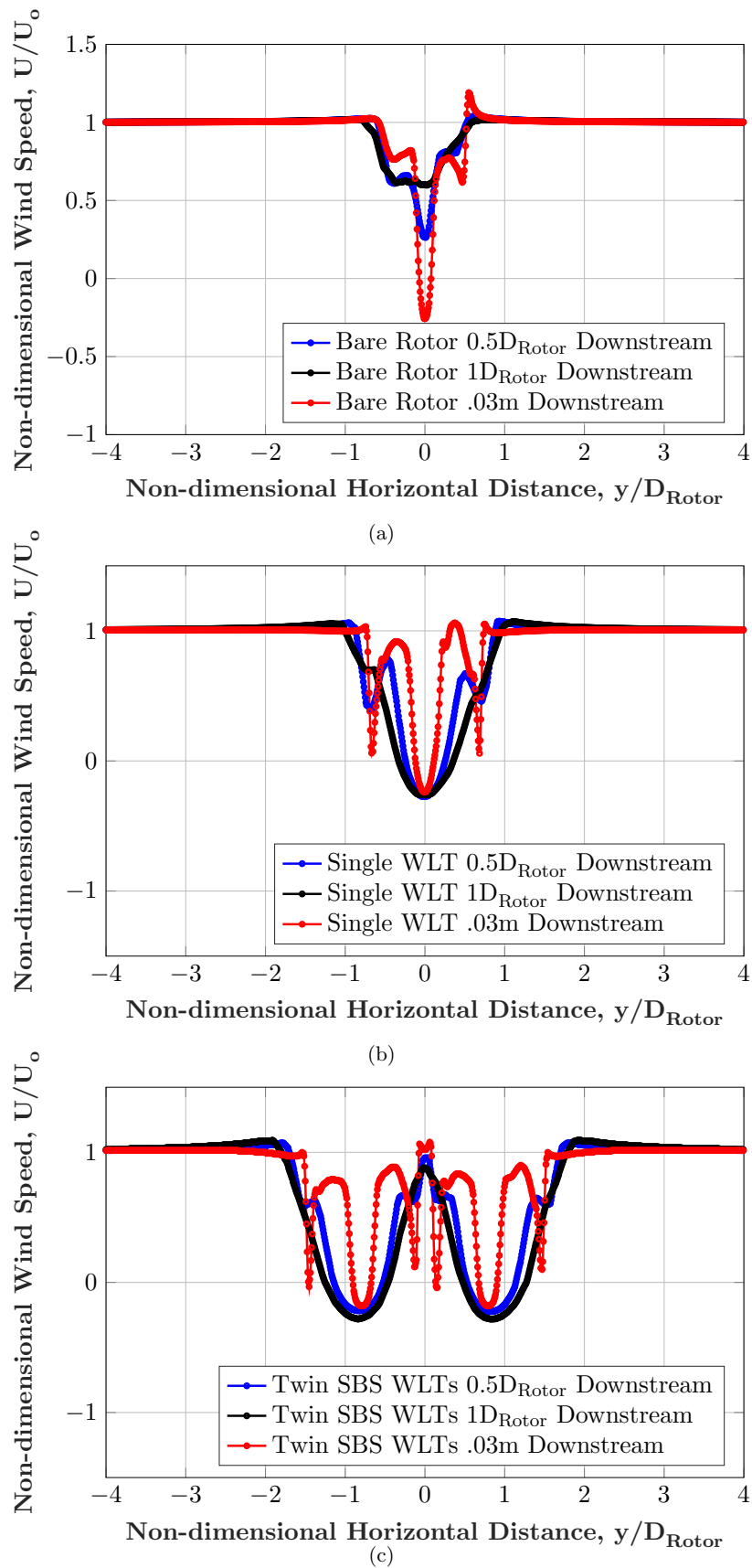


Figure 14: Comparisons of numerical u-velocity distributions at different downstream locations for bare rotor (a), single WLT (b), and twin SBS WLTs (c)

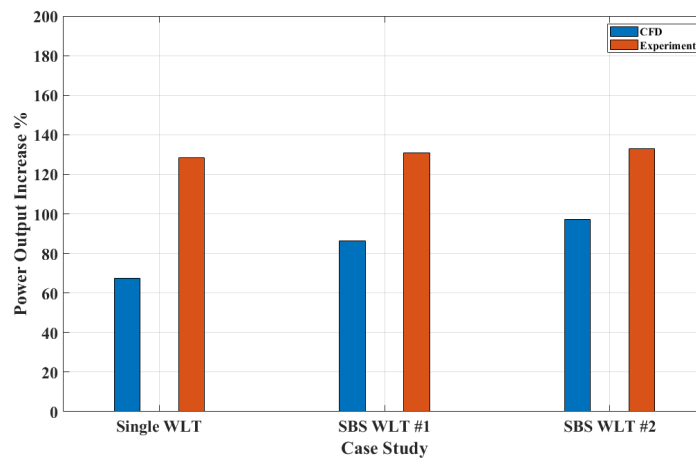


Figure 15: Comparison of power output increase for each case study relative to the bare rotor value

Consequently, the gap flow between WLTs in close vicinity plays an critical role to boost up the power coefficient. In order to better capture the wake structures, wake shedding and interaction between the two rotors, the current simulation is being upgraded to LES with fully resolved wind turbine blades. Then validation will be performed with the experimental data at a later publication.

4. Conclusions and Future Work

Multirotor systems for wind turbine configurations have been studied using both numerical and experimental approaches. A large wind tunnel in Kyushu University is used for all the experiments. In parallel with wind tunnel experiments, RANS CFD simulations were performed on bare rotor, single WLT, and twin SBS WLTs cases using fully resolved blades, based on FVM. The WLT obviously shows a large increase in power output compared to the bare rotor case. Besides, the twin SBS WLTs shows even larger power increase compared to the case of single WLT by around 20% for CFD calculations at the optimum tip speed ratio s/D of around 0.2. The increase in the power coefficient and the drag coefficient for the MRS configuration in close proximity can be explained by the flow interference around bluff bodies and gap flow behaviours. For all studied cases, RANS simulations showed good agreement in the power coefficient. The lowered pressure regions were due to the accelerated gap flows effect that leads to vortices near the gaps, and thus causing the lowered pressure region behind the twin SBS WLTs. This means, the lowered pressure region draws more airflow into the turbines in the MRS compared to the single WLT or bare rotor. Therefore, the power and drag values for MRS are higher compared to those of the stand-alone configurations. As the number of units for an MRS is increased, the increase in power output becomes larger and larger. This is because that the gap flows between brimmed diffuser-augmented wind turbines (B-DAWT) in a MRS are accelerated and cause lowered pressure regions due to vortex interaction behind the brimmed diffusers. Thus, a MRS with more B-DAWTs can draw more wind into turbines showing higher power output.

In order to obtain a better understanding of the wake structure, interference, and the interaction between the rotors, CFD simulations will be upgraded to LES then validated against the experimental data at a future publication. Besides, further studies are going to be performed on more WLTs up to 7 rotors both numerically and experimentally.

5. References

- [1] Jamieson, P., and Branney, M., 2012, “Multi-Rotors; A Solution to 20MW and Beyond?,” *Energy Procedia*, 24, pp. 52–59.
- [2] Heronemus, W., 1972, “Pollution-Free Energy From Offshore Winds,” Eighth Annual Conference and Exposition, Marine Technology Society, Washington, DC, Dec. 26–31.
- [3] Amano, R. S., 2017, “Review of Wind Turbine Research in 21st Century,” *ASME J. Energy Resour. Technol.*, 139(5), p. 050801.
- [4] Jamieson, P., and Branney, M., 2012, “Multi-Rotors; A Solution to 20MW and Beyond?,” *Energy Procedia*, 24, pp. 52–59.
- [5] Jamieson, P., 2018, *Innovation in Wind Turbine Design*, 2nd ed., Wiley, Chichester, UK.
- [6] Sieros, G., Chaviaropoulos, P., Sørensen, J. D., Bulder, B. H., and Jamieson, P., 2012, “Upscaling Wind Turbines: Theoretical and Practical Aspects and Their Impact on the Cost of Energy,” *Wind Energy*, 15(1), pp. 3–17.
- [7] Hofmann, M., and Sperstad, I. B., 2014, “Will 10MW Wind Turbines Bring Down the Operation and Maintenance Cost of Offshore Wind Farms?,” *Energy Procedia*, 53, pp. 231–238.
- [8] Heronemus, W., 1972, “Pollution-Free Energy From Offshore Winds,” Eighth Annual Conference and Exposition, Washington, DC, Dec. 26–31.
- [9] Smulders, P. T., Orbons, S., and Moes, C., 1984, “Aerodynamic Interaction of Two Rotors Set Next to Each Other in One Plane,” *European Wind Energy Conference*, Hamburg, Germany, Oct. 22–26, pp. 529–533.
- [10] Ransom, D., Moore, J. J., and Heronemus-Pate, M., 1984, “Performance of Wind Turbines in a Closely Spaced Array,” *Renewable Energy World*, 2(3), pp. 32–36.
- [11] Chasapogiannis, P., Prospathopoulos, J. M., Voutsinas, S. G., and Chaviaropoulos, T. K., 2014, “Analysis of the Aerodynamic Performance of the Multi-Rotor Concept,” *J. Phys: Conf. Ser.*, 524, p. 012084.
- [12] Yoshida, S., Goeltenbott, U., Ohya, Y., and Jamieson, P., 2016, “Coherence Effects on the Power and Tower Loads of a 72MW Multi-Rotor Wind Turbine System,” *Energies*, 9(9), pp. 742–757.
- [13] INNWIND.EU, 2017, “Deliverable 1.33 Innovative Turbine Concepts—Multi-Rotor System,” European Union, Brussels, Belgium, accessed Sept. 26, 2017, <http://www.innwind.eu/publications/deliverable-reports>
- [14] Ohya, Y., Miyazaki, J., Goltenbott, U., and Watanabe, K., 2017, “Power Augmentation of Shrouded Wind Turbines in a Multirotor System,” *ASME J. Energy Resour. Technol.*, 139(5), p. 051202.
- [15] Goltenbott, U., Ohya, Y., Yoshida, S., and Jamieson, P., 2017, “Aerodynamic Interaction of Diffuser Augmented Wind Turbines in Multi-Rotor Systems,” *Renewable Energy*, 112, pp. 25–34.
- [16] Watanabe, K., and Ohya, Y., 2018, “Multi-Rotor Systems Using Three Shrouded Wind Turbines for Power Output Increase,” *ASME J. Energy Resour. Technol.* (accepted).
- [17] Yuji, O., and Koichi, W. (2019). A new approach toward power output enhancement using multirotor systems with shrouded wind turbines. *Journal of Energy Resources Technology*, Transactions of the ASME, 141(5), [051203]. <https://doi.org/10.1115/1.4042235>
- [18] Watanabe, K., and Ohya, Y. (2019). Multirotor Systems Using Three Shrouded Wind Turbines for Power Output Increase. *Journal of Energy Resources Technology*, Transactions of the ASME, 141(5), [051211]. <https://doi.org/10.1115/1.4042971>

- [19] Ohya, Y., Miyazaki, J., Göltenbott, U., and Watanabe, K. (2017). Power Augmentation of Shrouded Wind Turbines in a Multirotor System. *Journal of Energy Resources Technology, Transactions of the ASME*, 139(5), [051202]. <https://doi.org/10.1115/1.4035754>
- [20] Halawa, A. M., Sessarego, M., Shen, W. Z., and Yoshida, S. (2018). Numerical Fluid-Structure Interaction Study on the NREL 5MW HAWT. *Journal of Physics: Conference Series*, 1037(2), [022026]. <https://doi.org/10.1088/1742-6596/1037/2/022026>
- [21] Ohya, Y., and Karasudani, T., 2010, “A Shrouded Wind Turbine Generating High Output Power With Wind Lens Technology,” *Energies*, 3(4), pp. 634–649.
- [22] Matsumiya, T., Kogaki, T., Iida, K., and Kieda, K., 21, “A Development of High Performance Aerofoil,” *Turbomachinery*, 29, pp. 519–524.
- [23] Ohya, Y., Okajima, A., and Hayashi, M., 1989, “Wake Interference and Vortex Shedding,” *Encyclopedia of Fluid Mechanics*, N. P. Cheremisinoff, ed., Vol. 8, Gulf Publishing Corporation, Houston, TX, pp. 323–389.
- [24] Ohya, Y., 2014, “Bluff Body Flow and Vortex—Its Application to Wind Turbines,” *Fluid Dyn. Res.*, 46(6), p. 061423.
- [25] Ohya, Y., Miyazaki, J., Göltenbott, U., and Watanabe, K., 2017, “Power Augmentation of Shrouded Wind Turbines in a Multirotor System,” *ASME J. Energy Resour. Technol.*, 139(5), p. 051202.

Acknowledgment

We gratefully acknowledge our laboratory staff, Ao Takada, Keiji Matsushima and David Carrillo for their cooperation and assistance in the experiments and in the analysis of the data. This research was supported by the New Energy and Industrial Technology Development Organization (NEDO), Japan, and by the Ministry of Education, Culture, Sports, Science and Technology-Japan (MEXT).